

# Luminescent solar concentrators with fiber geometry

Oreane Y Edelenbosch,<sup>1,2</sup> Martyn Fisher,<sup>2</sup> Luca Patrignani,<sup>2</sup>  
Wilfried G J H M van Sark,<sup>1</sup> and Amanda J Chatten<sup>2,\*</sup>

<sup>1</sup>*Copernicus Institute of Sustainable Development, Utrecht University, Budapestlaan 6, 3584 CD Utrecht, The Netherlands*

<sup>2</sup>*Department of Physics, Imperial College London, Prince Consort Road, London SW7 2AZ, UK*  
*\*a.chatten@imperial.ac.uk*

**Abstract:** The potential of a fibre luminescent solar concentrator has been explored by means of both analytical and ray-tracing techniques. Coated fibres have been found to be more efficient than homogeneously doped fibres, at low absorption. For practical fibres concentration is predicted to be linear with fibre length. A 1 m long, radius 1 mm, fibre LSC doped with Lumogen Red 305 is predicted to concentrate the AM1.5g spectrum up to 1100nm at normal incidence by  $\sim 35\times$ . The collection efficiency under diffuse and direct irradiance in London has been analysed showing that, even under clear sky conditions, in winter the diffuse contribution equals the direct.

©2013 Optical Society of America

**OCIS codes:** (350.6050) Solar energy; (220.1770) Concentrators; (250.5230) Photoluminescence.

---

## References and links

1. International Energy Agency, Solar Energy Perspectives. OECD/IEA, (2012).
2. E. E. Bende, A. R. Burgers, L. H. Slooff, W. G. J. H. M. van Sark, and M. Kennedy, "Cost and Efficiency Optimisation of the Fluorescent Solar Concentrator," in *Proceedings of the 23rd European Photovoltaic Solar Energy Conference*, G. Willeke, H. Ossenbrink, P. Helm, eds. (WIP-Renewable Energies, Munich, Germany, 2008), pp. 461–469.
3. W. G. J. H. M. van Sark, K. W. J. Barnham, L. H. Slooff, A. J. Chatten, A. Büchtemann, A. Meyer, S. J. McCormack, R. Koole, D. J. Farrell, R. Bose, E. E. Bende, A. R. Burgers, T. Budel, J. Quilitz, M. Kennedy, T. Meyer, C. M. Donegá, A. Meijerink, and D. Vanmaekelbergh, "Luminescent Solar Concentrators--a review of recent results," *Opt. Express* **16**(26), 21773–21792 (2008).
4. A. Goetzberger and W. Greube, "Solar Energy Conversion with Fluorescent Collectors," *Appl. Phys. (Berl.)* **14**(2), 123–139 (1977).
5. W. H. Weber and J. Lambe, "Luminescent greenhouse collector for solar radiation," *Appl. Opt.* **15**(10), 2299–2300 (1976).
6. K. McIntosh, N. Yamada, and B. S. Richards, "Theoretical comparison of cylindrical and square-planar luminescent solar concentrators," *Appl. Phys. B* **88**(2), 285–290 (2007).
7. G. Colantuono, A. Buckley, and R. Erdélyi, "Ray-Optics Modelling of Rectangular and Cylindrical 2-Layer Solar Concentrators," *J. Lightwave Technol.* **31**(7), 1033–1044 (2013).
8. R. H. Inman, G. V. Shcherbatyuk, D. Medvedko, A. Gopinathan, and S. Ghosh, "Cylindrical luminescent solar concentrators with near-infrared quantum dots," *Opt. Express* **19**(24), 24308–24313 (2011).
9. D. J. Farrell, "PVtrace optical ray tracing for photovoltaic devices and luminescent materials," (2012). <https://github.com/danieljfarrell/pvtrace>, accessed 19 January 2013.
10. D. J. Farrell, PhD Thesis, "Characterising the Performance of Luminescent Solar Concentrators," University of London, 2008.
11. [www.python.org](http://www.python.org), accessed 19 January 2013.
12. A. J. Chatten, D. J. Farrell, R. Bose, A. Dixon, C. Poelking, K. C. Gödel, M. Mazzer, and K. W. J. Barnham, "Luminescent and Geometric Concentrators for Building Integrated Photovoltaics," in *Proceedings of 37th IEEE Photovoltaic Specialists Conference* (Institute of Electrical and Electronics Engineers, New York, 2011), pp. 852–857.
13. R. Bose, D. J. Farrell, A. J. Chatten, M. Pravettoni, A. Büchtemann, J. Quilitz, A. Fiore, L. Manna, J. H. Nelson, A. P. Alivisatos, and K. W. J. Barnham, "The Effect of Size and Dopant Concentration on the Performance of Nanorod Luminescent Solar Concentrators," in *Proceedings of the 23rd European Photovoltaic Solar Energy*

- Conference*, G. Willeke, H. Ossenbrink, P. Helm, eds. (WIP-Renewable Energies, Munich, Germany, 2008), pp. 552–555.
14. A. J. Chatten, K. W. J. Barnham, B. F. Buxton, N. J. Ekins-Daukes, and M. A. Malik, “Quantum Dot Solar Concentrators,” *Semiconductors* **38**(8), 909–917 (2004).
  15. M. Kennedy, A. J. Chatten, D. J. Farrell, R. Bose, A. Büchtemann, S. J. McCormack, J. Doran, K. W. J. Barnham, and B. Norton, “Luminescent solar Concentrators: A Comparison of Thermodynamic Modelling and Ray-trace Modelling Predictions,” in *Proceedings of the 23rd European Photovoltaic Solar Energy Conference*, G. Willeke, H. Ossenbrink, P. Helm, eds. (WIP-Renewable Energies, Munich, Germany, 2008), pp. 334–337.
  16. L. R. Wilson and B. S. Richards, “Measurement method for photoluminescent quantum yields of fluorescent organic dyes in polymethyl methacrylate for luminescent solar concentrators,” *Appl. Opt.* **48**(2), 212–220 (2009).
  17. V. Sholin, J. D. Olson, and S. A. Carter, “Semiconducting polymers and quantum dots in luminescent solar concentrators for solar energy harvesting,” *J. Appl. Phys.* **101**(12), 123114 (2007).
  18. Z. Krumer, S. J. Pera, R. J. A. van Dijk-Moes, Y. Zhao, A. F. P. de Brouwer, E. Groeneveld, W. G. J. H. M. van Sark, R. E. I. Schropp, and C. de Mello-Donagá, “Tackling self-absorption in Luminescent Solar Concentrators with type-II colloidal quantum dots,” *Sol. Energy Mater. Sol. Cells* **111**, 57–65 (2013).
  19. C. Gueymard, “SMARTS2, simple model of the atmospheric radiative transfer of sunshine: algorithms and performance assessment,” Report FSEC-PF-270–95, Florida Solar Energy Center, Cocoa, FL, 1995.
  20. A. Goetzberger, “Fluorescent Solar Energy Collectors: Operating Conditions with Diffuse Light,” *Appl. Phys. (Berl.)* **16**(4), 399–404 (1978).
- 

## 1. Introduction

The Sun is an abundant, climate friendly, inexhaustible energy source, available in every country and in particular in those countries which are expected to experience high economic and population growth in the coming decades [1]. However, converting the energy of the Sun at a high efficiency, and especially in a way that can compete economically with conventional energy sources, remains difficult to achieve.

One approach to lower cost per installed capacity is by concentrating the sunlight before it reaches the solar cell and, when concentrating up to 100 suns, the heat flux is still low and no active cooling is needed. A luminescent solar concentrator (LSC), consisting of a transparent polymer waveguide doped with luminescent species (see Fig. 1), has the ability to concentrate solar photons in this low concentration range, while also down-shifting the energy of the photons so that even less heat is dissipated in the solar cells the LSC is coupled to. The luminescent species generally emit isotropically, and a significant part is trapped by total internal reflection (TIR) and waveguided to the edges. The area-ratio of the top surface where the photons are incident to the edges results in concentration of the light. As the cost of transparent polymers such as a poly methyl methacrylate (PMMA) is low compared to that of a solar cell [2], using an LSC can decrease the overall cost of the photovoltaic (PV) electricity production [3].

Flat plate LSCs were first developed in the late 1970s [4,5] and, although development stalled owing to the lack of stable, highly luminescent dyes, there has been renewed interest in the LSC application over the last decade as new and stable luminescent species have become available. However, to date LSCs have not been commercially viable, primarily because the optical efficiency remains too low. As a response, McIntosh recently proposed a new geometry, the cylindrical LSC, which is estimated to be 1-1.9 times as efficient [6] as a flat plate LSC. This result has evoked questions on the applicability and optimal characteristics of the cylindrical LSC, see also [7,8].

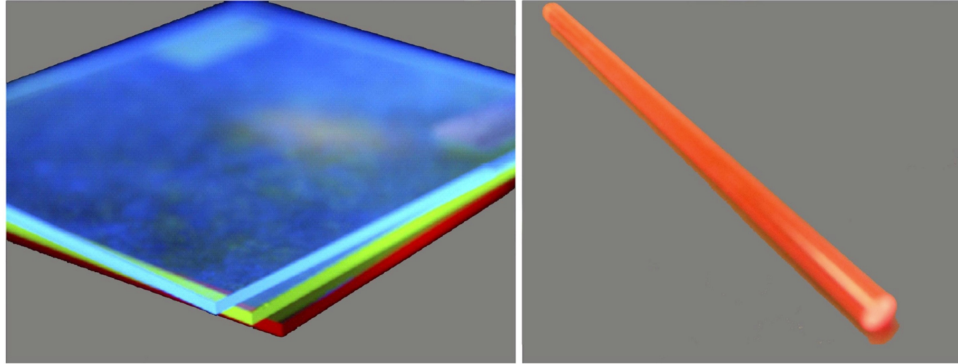


Fig. 1. Luminescent solar concentrators with flat plate and cylindrical geometries.

The characteristic of a cylinder is that the longer and thinner it is, the larger the area-ratio between the illuminated surface and the edges. Following this reasoning an LSC with fiber geometry should have a large concentrating potential. As optical and polymer fibers are already produced on large scales, manufacturing processes for these fibers are well known. The production steps are optimized, resulting in low host material losses and low manufacturing cost. At the same time fibers have the advantages that they are light-weight and are flexible. By analyzing the interactions between the solar photons and the fiber, and investigating different configurations, a better understanding of the working mechanism of this type of LSC can be gained.

## 2. Ray-trace modelling of fiber LSCs

The flexible ray-tracing software PVtrace [9,10] written in PYTHON [11] and developed at Imperial College London was used to simulate the behavior of photons travelling through the fiber LSCs. The program traces individual photon paths through the LSC and uses Monte Carlo methods to assign the outcome of events that the photon may experience. A few examples of such events are: whether a photon is absorbed and where, whether the photon is emitted and with what direction and wavelength. The input to the program consists of absorption and emission data of the luminescent material, the direction and spectrum of the photon source, the loss coefficient of the host material and the geometry of the LSC. After having encountered an event a photon is labeled and when the simulation is complete, a database can be interrogated to determine the number of photons with a certain label, e.g. the number of absorbed photons exiting one end of the fiber LSC.

### 2.1 Verification of the ray-trace model

PVtrace has been verified against experimental measurements on a cylindrical LSC consisting of an off-center Lumogen red 305 dye doped cylindrical PMMA core within an outer transparent PMMA cylinder [12]. This design was optimized for secondary concentration of light concentrated by linear Fresnel lenses in a high concentration power generating window system. Although the design of the cylindrical LSC in that study and the dimensions (radius 10 mm, length 47 cm) were somewhat different to those in the present study, the excellent agreement between the simulated ( $8.52 \pm 0.12\%$ ) and measured ( $8.30 \pm 0.97\%$ ) optical efficiencies for this larger cylindrical LSC (with an air-gap, diffuse, PTFE reflector), comprised of the same materials as used here, give confidence in the results presented in this study.

In addition, an earlier ray-tracer, written in C++ (see e.g [13].), also developed at Imperial College and their fundamental thermodynamic 3D flux model for flat plate LSCs (see e.g [14].) are compared with PVtrace for a homogeneously doped flat plate LSC in [12]

and results are shown to agree to within 1% giving further confidence in the results of this work. The thermodynamic 3D flux model has also been compared to the ray-tracer developed at ECN in [3] as well as being compared to the ray-tracer developed by DIT in [15] and agreement to within 1% was again found in all cases. All these models have been extensively verified against experimental measurements, (see [3, 10–15] and references therein) giving confidence that the conclusions of this modelling study will prove robust.

## 2.2 Scope of the study

In the first part of this study the AM1.5g spectrum up to 1100 nm (equaling the bandgap of Si) at normal incidence was used as the illumination source. Multicrystalline Si solar cells currently dominate over other materials in terms of global installed capacity and, we assume that for cost reasons, the fiber LSC is coupled to Si cells. With Si cells photons with a wavelength >1100 nm will not have enough energy to excite carriers across the bandgap and will not contribute to the electrical power production. Thus the optical efficiency and effective photon concentration values presented here are calculated up to 1100 nm only; when taking the whole solar spectrum into account the values would be lower.

Lumogen Red 305 (see Fig. 2(a)) is a standard, stable luminescent dye suitable for doping LSCs and was used in this study. In the simulations it was assumed that the PMMA host loss coefficient is  $0.3 \text{ m}^{-1}$  and the luminescence quantum yield of the dye is 1 (it has been measured at 0.98–1.00 [16]).

As discussed in [6], and unlike the case of a flat plate, in a cylinder the trapping probability depends on the position of the emission event with respect to the center of the cylinder. For a refractive index  $n = 1.5$  and isotropic emission the trapping probability is ~33% for emission at the center of the cylinder and increases towards the outer hull of the cylinder reaching a value of ~74%, identical to that of a flat plate. It is therefore expected that coated fibers, which only have a dye doped layer at the outer surface, will be more efficient than homogeneously doped fibers because more photons will be trapped. In this first part of the work homogeneously doped and coated fibers of radius  $r = 1 \text{ mm}$ , and length  $l = 10 \text{ cm}$ , were compared as the dye concentration was varied. For the coated fibers the dye-doped coating was 0.05 mm thick.

The fiber length and radius were varied to get a better understanding of absorption and re-absorption processes. Re-absorption of emitted photons over the wavelength range of overlap of the absorption and emission (see Fig. 2(a)) leads to significant losses (>50% for practical  $l \sim 40 \text{ cm}$ , flat plate LSCs [3]) by providing further opportunities for photons to be lost on emission at angles to the surface normal less than that required for trapping. It has also been shown [10,13,17] that for flat plate LSCs re-absorption limits the useful size of the LSC to less than 1m as additional re-absorption losses cause the concentration to plateau as the lateral dimensions are increased. However, type-II colloidal quantum dots [18] and the conjugated polymer Red F [17], both with large Stokes' shift have been demonstrated to mitigate self-absorption in flat plate LSCs. An aim of this study was to determine whether re-absorption is a limiting factor for practical fiber LSCs.

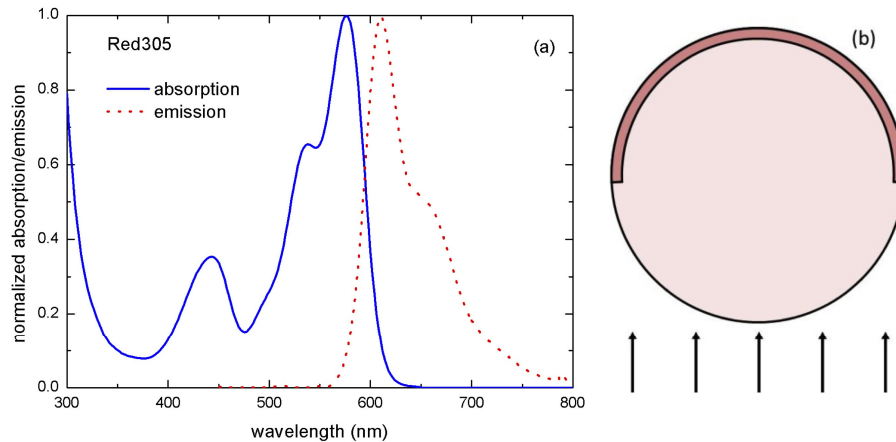


Fig. 2. (a) Normalized absorption and emission spectra of Lumogen F Red 305. (b) Schematic picture of the half coated fiber. The red colored area is the area, which is coated in our simulations.

In the next part of the study a half coated fiber (see Fig. 2(b)) has been simulated, where the coated layer was 0.05 mm thick. Refraction changes the direction of the incident photons on entering the fiber following Snell's equation due to the curved surface of the fiber. For a single angle of incidence as would be the case for direct sunlight, the light is focused to a small region on the backside of the fiber. However, to fully capture diffuse sunlight (assumed isotropic over a hemisphere) half the fiber would need to be coated. Following this the effect of multiple fibers is investigated with the aim of understanding what fractions of the transmitted incident photons and those emitted photons lost from the LSC can be recycled by neighboring fibers.

The aim of the final part of this study was to determine realistic operating parameters for fiber LSCs installed in London and investigate how the diffuse and the direct insolation contribute to it.

In order to obtain statistically significant results the paths of at least 10,000 photons were tracked through the simulated fibers, and characteristics such as the optical efficiency, the effective photon concentration, as well as the percentages of photons absorbed and re-absorbed, were determined.

In all the simulations we assumed no refractive index mismatch at the ends of the fiber. This approximates the case for PV cells attached to the fiber ends with an adhesive matched to that of the PV cell's cover glass. The adhesive could therefore potentially be PMMA itself, which with its refractive index of  $\sim 1.5$  is a good match to most glasses. However there may be thermoplastics or sol-gel materials, which have superior adhesive properties to PMMA. Whatever the specifics of the PMMA, adhesive and the cover glass the refractive index mismatches are likely to be small and cause minimal reflection losses back into the fiber.

### 3. Coated and homogeneous fibers

To absorb the same amount of photons the coated fiber must have a higher optical density than the homogeneous fiber, as the path length through the dye is shorter. To make a fair comparison the fiber properties are compared at dye levels for which they have equal light harvesting potential and absorb the same fraction of the incident photon flux (see Fig. 3).

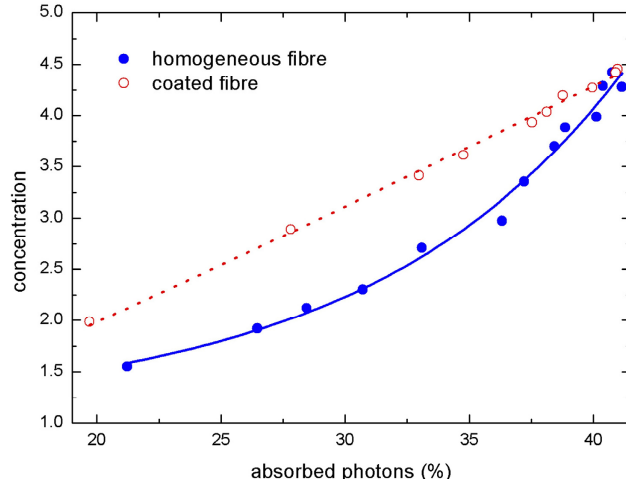


Fig. 3. Optical concentration of a coated and a homogeneous fiber while varying the dye absorption coefficient (number of photons absorbed).

### 3.1 Varying solar photon harvesting

The photon concentration is the product of the optical efficiency,  $\eta_{\text{opt}}$ , and geometric area-ratio  $G$ . For conversion by PV cells on both ends of the fiber LSC  $G = lr/\pi r^2$  and  $\eta_{\text{opt}}$  is defined as the ratio of the photons collected per unit PV area to those incident per unit LSC collection area. As can be seen in Fig. 3 for the lower fractions of absorbed photons,  $\eta_{\text{opt}}$  and thus the photon concentration, is higher using the coated fiber than the homogeneous fiber.

Increasing the optical density in a homogeneous fiber (by increasing the dye concentration), will cause more photons to be absorbed at an earlier stage towards the outer hull and ultimately the homogeneous fiber will act exactly the same as a coated fiber. Therefore, at high absorption the coated fiber and the homogeneous fiber approach the same concentration value (see Fig. 3). A limiting photon concentration value is reached beyond which no further absorption gains or re-absorption losses can take place. This can be explained by multiple re-absorptions taking place on length scales shorter than the fiber length so the photons propagating along the fiber are so red-shifted that they can effectively no longer be further re-absorbed. This effect occurs because, in order to satisfy energy conservation, after absorption (or re-absorption) and emission (or re-emission) the photon has a lower energy (a red-shifted, longer wavelength).

It is expected that when using other luminescent materials than Lumogen Red 305 the coated fiber would still be more efficient compared to the homogeneous fiber since the higher trapping efficiency attained depends on the location of the absorbing material and not on the absorption or emission spectra.

In order to put the fractions of AM1.5g photons absorbed into perspective a peak absorption coefficient of  $23,000 \text{ m}^{-1}$  corresponds to a dye concentration of around 4% by mass in PMMA and for the  $r = 1 \text{ mm}$  diameter homogeneous fiber this corresponds to absorbing 37% of the incident photons in the range 300 to 1100 nm. In practice it is difficult to fully disperse the dye in PMMA at this level as dye agglomeration starts to become a significant problem, owing to significant scattering, whereas at a concentration of 2% by mass (equivalent to a peak absorption coefficient  $\sim 11,000 \text{ m}^{-1}$ ) no agglomeration is seen. However, the photon harvesting achieved by the higher absorption coefficients used in this simulation study, which would provide for optimal concentration albeit with slightly reduced optical efficiency, could be achieved for the coated geometry by thermal evaporation of the dye rather than by using coating or casting methods.

In order to increase the photon harvesting beyond the ~40% limit (for AM1.5g in the range 300 to 1100 nm) for Lumogen Red 305 (see Fig. 3) it would be possible to fabricate fiber LSCs containing multiple dyes or use another type of sensitizer such as inorganic semiconductor nanoparticles (see e.g [3,8,13,14,17,18]). For flat plate LSCs stacked layers containing different absorbers can be envisaged each attached to a PV cell with an optimal bandgap, as originally proposed by Goetzberger and Greubel [4]. This configuration, which allows optimization of the power conversion efficiency by reducing thermalization losses in a similar way to multijunction cells, would be more difficult to fabricate for the cylindrical geometry as it would require concentric cylinders with air gaps between them and appropriately shaped PV cells. However, such stacked devices are unlikely to be cost effective because adding a second layer doubles the cost but is unlikely to ever double the efficiency.

### 3.2 Re-absorption in the fiber

To achieve a better understanding of re-absorption processes and to compare these processes taking place in both fiber designs the percentage of the absorbed photons absorbed once, twice, three times or more than three times have been calculated (see Fig. 4.). In the homogeneous fiber maximum re-absorption has not taken place at 21% photons absorbed. Increasing the optical density causes the amount of photons absorbed once to decrease and the amount of photons absorbed twice or more to increase. When the total fraction of photons absorbed is around 40%, maximum re-absorption has taken place and the percentages of photons absorbed once and more do not change on further increasing the optical density.

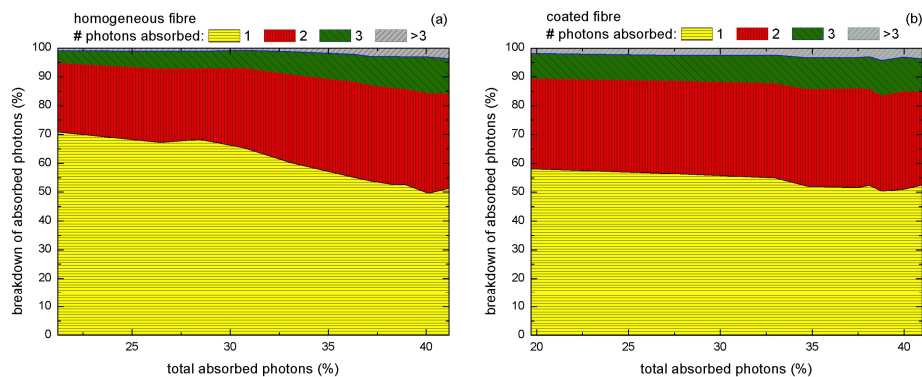


Fig. 4. Of the photons absorbed, the percentages absorbed once, twice, three and more than three times for the homogeneous (a) and coated (b) fiber.

In Fig. 4 it can be seen that a greater amount of re-absorption occurs in the coated fiber at a lower fraction of photons absorbed. An explanation for this difference can be found in the discovery that a larger fraction of the photons emitted close to the surface are oblique rays that follow a helical path where they spiral along the hull surface of the cylinder [6]. The path length that they then have to travel to reach the ends of the fiber can be many multiples of the fiber length. Since photon absorption depends on the path length and on the optical density, according to the Beer-Lambert law, in a coated fiber more re-absorption occurs in a shorter fiber length. However, despite this greater re-absorption the results of the previous section show that, since the coated fiber is slightly more efficient than the homogeneous one, the benefits of greater trapping in a coated fiber outweigh these losses due to higher re-absorption until the very high optical density regime where the fiber is absorbing >40% and both configurations show the same behavior.

### 3.3 Varying fiber length and radius

The results of the preceding section indicate that at high optical density increasing the length of the fiber will not induce further re-absorption losses as the maximum possible re-absorption has already occurred and, as discussed above, the photons that propagate within the fiber are those that are so red-shifted that the chance they will be further re-absorbed by the dye (wavelength  $> 650$  nm, see Fig. 2(a)) is vanishingly small. The geometrical concentration  $G$  will however increase, which should result in higher photon concentrations in contrast to the case for flat plate LSCs where the concentration plateaus as the size is increased as discussed above. To analyze whether this is the case homogeneous and coated fibers, with  $r = 1$  mm, and lengths up to 1 meter have been modelled.

In addition, homogeneous fibers with  $l = 10$  cm have been modelled for  $r = 0.5$  mm and 2 mm. When the radius is larger more photons can be absorbed when passing through the fiber but at the same time a larger radius will result in a lower geometric ratio  $G$ . In Fig. 5 the photon concentration and optical efficiency is plotted against the size change for both dimensions.

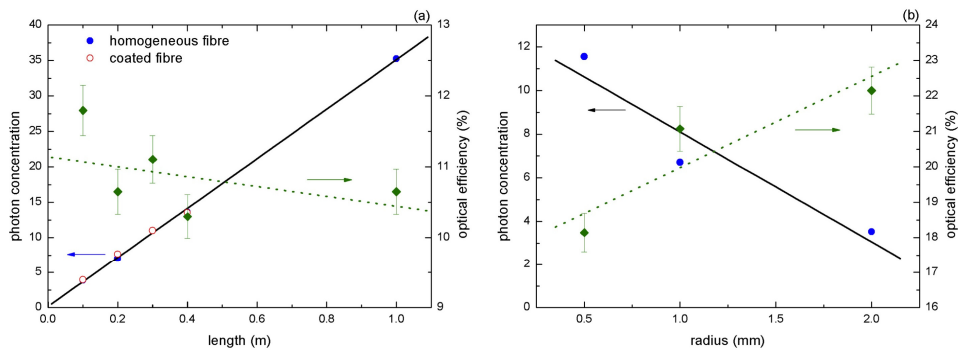


Fig. 5. (a) Photon concentration and optical efficiency of a coated and a homogeneous fiber while varying the length  $l$ . Peak absorption coefficients of  $2300\text{ m}^{-1}$  for the homogeneous fiber and  $23000\text{ m}^{-1}$  for the coated fiber were used. (b) Concentration and optical efficiency of a homogeneous fiber while varying the radius  $r$ . The absorption coefficient for all three fibers was  $23000\text{ m}^{-1}$ , which corresponds to 35%, 37% and 40% of photons absorbed for the 0.5, 1.0 and 2.0mm radius fibers respectively.

For the study of the effect of fiber length (Fig. 5(a)) the dye absorption coefficients for the two configurations were chosen such that for the  $l = 10$  cm fibers the photon concentrations were equal at around  $12x$ . As seen in Fig. 5(a), and in agreement with the hypothesis above the concentration increases linearly with fiber length since the maximum re-absorption loss occurs within a relatively short length of fiber. Consistent with this observation  $\eta_{\text{opt}}$  only drops from 11.8% to 10.3% on increasing the fiber length from 10 to 40 cm. The efficiency drop is thus mostly the result of an increase in host absorption losses on increasing the length. The effective photon concentration for a 1 m length of this fiber (with Si cells at the ends) is predicted to be around  $35x$  showing that using long fibers has a huge potential. As shown in Fig. 5(b)  $\eta_{\text{opt}}$  increases from 17% to 21% when increasing the radius of the fiber from 0.5 mm to 2 mm. This increase in optical efficiency is due to the increased fraction of incident photons absorbed as the path length crossing the fiber is longer. This optical efficiency increase depends on the optical density of the material. If the optical density is high and maximum absorption has taken place, the radius size increase will not induce extra absorption. For the dye peak absorption coefficient chosen for this study the overall concentration decreases when changing the radius from 0.5 mm to 2 mm because the optical efficiency gain is smaller than the reduction in geometric ratio  $G$ .

#### 4. Half coated fiber and multiple fiber arrays

In Fig. 6 the photon concentration of the half coated fiber (see Fig. 2(b)) and fully coated fiber are compared, again with respect to the fraction of incident photons absorbed. Less of the cross sectional area in the half coated fiber is doped with organic dye which, it was initially thought, would result in lower re-absorption losses compared with the fully coated fiber since photons propagating along the fiber LSC will spend a smaller fraction of their path-length within the dye doped regions.

From Fig. 6(a) it can be seen that this is in fact not the case. The half coated, and the fully coated configurations are approximately equal (to within the simulation uncertainty). The explanation is again that for the optical densities considered, the re-absorption losses are already at nearly their maximum level, consistent with the results depicted in Fig. 4(b). For future research it would be interesting to repeat the study with a lower optical density. Although the difference between the configurations is negligible, the half-coated design would offer cost benefits as it uses half the luminescent material.

Next we considered a configuration of five coated fibers lying next to one another, with a mirror placed at the back of the array and the source light incident on only the fiber lying in the middle of the bundle. The aim was to understand what fraction of the light lost from a fiber (either incident light that remains unabsorbed after a first pass through the array or emitted light that is lost at escaping angles) can be recycled by near neighbor fibers. Figure 6(b) shows the results for diffuse (Lambertian) and specular mirrors with reflectivity  $R = 95\%$ . It is interesting to see that the neighboring fibers can indeed collect a few photons that would be otherwise lost and therefore an array of fibers gives a slightly higher optical efficiency than is achieved for isolated fibers. If all the fibers were exposed to sunlight then their optical efficiency would increase by  $\sim 1\%$  from their nearest neighbors and  $\sim 0.1\%$  from their next nearest neighbors. The mirror type does not appear to be critical and the reflectivity of 95% used in the simulations can be achieved for either type using PTFE as a diffuse reflector [10] or a commercially available specularly reflecting mirror foil [3] as required.

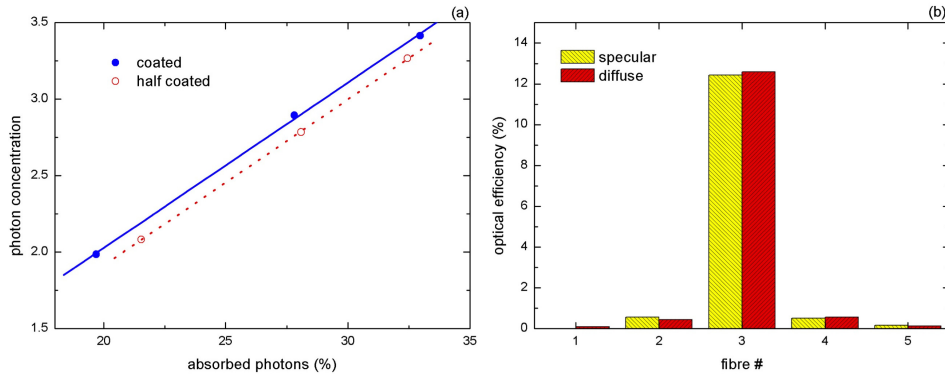


Fig. 6. (a) Photon concentration of half coated and fully coated fibers ( $r = 1\text{mm}$ ,  $l = 10\text{cm}$ ). (b) Simulations of an array of coated fibers with peak absorption coefficient of  $23000\text{ m}^{-1}$  showing the fractions of photons lost from the central fiber that are recycled by neighboring ones.

These simulations were for the AM1.5g spectrum at normal incidence but at other angles there will be losses due to shading of fibers by their nearest neighbors and quantifying these will be objective of further studies.

#### 5. Spectral modelling

In order to determine realistic operating parameters for this type of fiber LSC installed in London the programme SMARTS 2.9.5 [19] was used to simulate clear sky diffuse and direct

spectra in London on the solstices (21st of June and 22nd of December 2011) for every hour of the day (GMT is used). The data was converted to photon flux per wavelength and used as the source spectrum. The aim was to investigate how the diffuse and direct fractions of sunlight contribute to the LSC output with the solstices chosen as limiting cases.

To model the incident light realistically the angle of incidence was taken into account. For the direct light the fiber was simulated on a horizontal surface and was oriented with its long axis parallel to the North–south direction such that the cosine of the angle  $\beta$  between the axis of the fiber and the Sun is  $\cos\beta = \cos\alpha \cos A$  where  $\alpha$  is the solar altitude angle and  $A$  the solar zenith angle. This served to define the angle of incidence of the direct insolation and the diffuse insolation was assumed to be isotropic over a hemisphere. A homogeneous fiber with  $r = 1$  mm,  $l = 10$  cm and doped with dye such that the peak absorption coefficient is  $6400 \text{ m}^{-1}$  was simulated and the results are illustrated in Fig. 7.

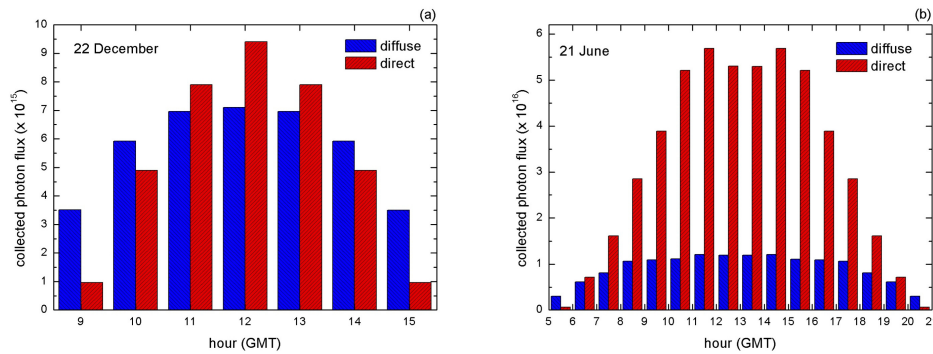


Fig. 7. Photon fluxes collected at the ends of the fiber for diffuse and direct sunlight on 22nd December (a) and 21st June (b). Note the difference in the vertical scales.

It can be seen that in winter the diffuse spectrum delivers a higher contribution at the beginning and the end of the day and overall the photons collected coming from the diffuse is quite similar to that coming from the direct. The optical collection efficiency for photons in the range 300–1100 nm is 21% for the diffuse and 9% for the direct and the effective photon concentrations are 6.8x and 2.9x respectively. This is because short wavelength light is scattered more effectively in the atmosphere so the diffuse spectrum is blue rich and can be better harvested by the LSC. This can be seen in the spectra themselves shown in Fig. 8 which shows the diffuse light to peak at  $\sim 500$  nm, which is within the absorption band of the dye, whereas the direct light peaks at  $\sim 800$  nm which is outside the dye absorption band.

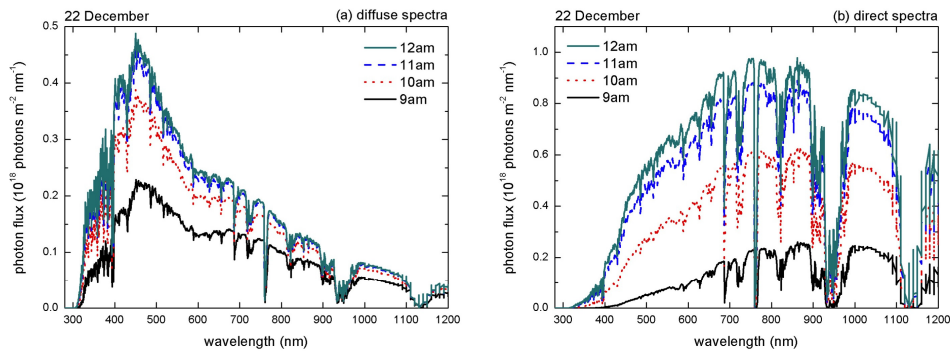


Fig. 8. Hourly diffuse (a) and direct (b) spectra for London on 22nd December. Note, only morning spectra are shown, as afternoon spectra are identical to morning ones, e.g., 1pm spectrum equals 11 am spectrum, etc.

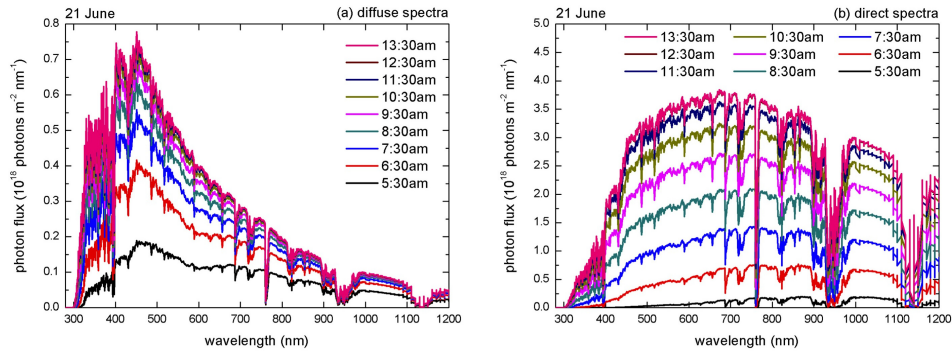


Fig. 9. Hourly diffuse (a) and direct (b) spectra for London on the 21st June. Note, only half of the daily spectra are shown.

In the summer the photon fluxes are higher and the angle between the rays and the fiber less steep with the result that  $\sim 5$  times as many photons are collected compared to in winter. The optical collection efficiency is 25% for the diffuse and 12% for the direct and the effective concentrations are 7.8x and 3.8x respectively. The summer spectra are illustrated in Fig. 9, showing again why the diffuse light is harvested with a higher efficiency since the diffuse peaks at  $\sim 450$  nm and the direct at  $\sim 750$  nm.

These data are for fibers just 10 cm in length and the effective concentration values would be far greater for longer fibers (see section 3.3). These results are also limited to clear sky spectra when the direct contribution dominates, but it is well known [20] that at high latitudes the diffuse outweighs the direct over the year and it is in these regions the LSC is most applicable.

## 6. Conclusions

A ray tracing approach has been used to increase our understanding of the working mechanisms in the fiber LSC and optimize the effective concentration potential. A significant result obtained as a result of this study is that, when comparing homogeneous and coated fibers that absorb equal numbers of photons, the coated fiber is indeed more efficient than the homogeneous in the regime of low photon absorption. When the absorption coefficient is high and many photons are absorbed, maximum re-absorption takes place within a relatively short length of fiber. Therefore increasing the length of the fiber does not induce more re-absorption but it does increase the geometrical concentration. Our results show that the increase in geometrical concentration is larger than the loss due to host absorption and scattering, and thus increasing the length of the fiber has the potential to increase the effective photon concentration well beyond that achieved by flat plate LSCs. In contrast to flat plate LSCs the concentration does not plateau with increasing solar collection area. A 1 m long fiber LSC doped with Lumogen Red 305 with  $r = 1$  mm is predicted to concentrate the AM1.5g spectrum up to 1100 nm at normal incidence by  $\sim 35$ x.

For the same fractions of incident photons absorbed the half coated fiber has the same optical efficiency as the coated fiber. It was initially expected that the half coated fiber would experience less re-absorption losses and therefore be more efficient but since near maximum re-absorption takes place, this effect is not visible in our simulations.

It can be concluded that high concentration is possible when using fiber LSCs, especially when using long coated fibers. Using fibers will induce high re-absorption losses as the length that the photons have to travel to the ends is relatively far. This is compensated by the high geometrical concentration of this configuration. Maximizing the absorption and geometrical concentration by tuning the length and the radius and reducing the escape cone losses by

placing the dye close to the surface are characteristics that play the most important role when applying an LSC fiber to concentrate sunlight.

The spectral modelling illustrates the importance of the diffuse component of sunlight when using Lumogen Red 305 as the luminescent light harvesting species. Therefore we conclude that LSCs doped with this dye are best deployed at high latitudes where the diffuse component of sunlight is >50% over the year and the low insolation requires that costs are kept low. A highly efficient luminescent species that absorbs into the NIR and has emission just below the bandgap of Si could almost double LSC efficiencies. Unfortunately organic materials that absorb into the NIR usually have low LQYs (generally below 50%) as phonons lying close in energy to the luminescent transition provide a mechanism for dissipation of the excitation energy as heat. Organometallic or nanocrystalline materials may provide a solution but these also usually have lower LQY (up to ~80%) compared to the near unity values seen for organic dyes.

### **Acknowledgments**

Special thanks go to Imperial College London for hosting this research. Funding for this research was supplied by an ERASMUS Placement grant.